Progress In Electromagnetics Research M, Vol. 75, 159–166, 2018

Accurate Evaluation of the Conductor Loss in Rectangular Microstrip Patch Reflectarrays

Sembiam R. Rengarajan[1, *] and Richard E. Hodges[2]

Abstract—In the moment method solution of the integral equations for currents of a rectangular microstrip patch reflectarray, the Leontovich boundary condition is employed to determine the conductor loss. If the basis functions contain edge conditions that approach infinity, the moment matrix elements will have diverging integrals in the Galerkin technique. In this paper, we present a criterion to stop the evaluation of these integrals at a distance before the edge, thereby avoiding the divergence problem. The stopping distance derived here is found to work for a range of values of permittivity, loss tangent, and thickness of the substrate, polarization, angles of incidence of the plane wave source, and also for superstrates. Our computed results are in good agreement with measured results and those computed by HFSS.

1. INTRODUCTION

The design and analysis of reflectarray antennas generally employ an approximate model of an infinite array excited by a plane wave based on local periodicity. The induced currents in the unit cell patch are usually formulated in terms of integral equations and solved by the method of moments (MoM) [1]. A previous work showed that for a rectangular patch, a single basis function with uniform distribution across the current direction and a half sinusoidal variation with an edge condition approaching zero along the current direction in MoM, referred to as MoM_1 in this paper, yields good results for the reflection coefficient [2]. For a very accurate evaluation of the phase of the reflection coefficient, especially for small values of the substrate thickness, a set of basis functions exhibiting even and odd variations and edge conditions approaching zero in the current direction and infinity across the current direction in the MoM solution, referred to as MoM_2 here, is required [2]. In both cases, the Galerkin procedure was employed.

The conductor loss in thin microstrip elements is evaluated in the moment method by using the well-known Leontovich boundary condition wherein one equates the total tangential electric field to the intrinsic impedance of the metal times the surface current [3, 4]. Application of a Galerkin formulation then yields moment matrix elements containing the inner product of identical basis and testing functions, resulting in diverging integrals when edge currents such as those in MOM_2 approach infinity. In prior work, conductor loss could not be incorporated because of these divergent integrals [2]. Lewin encountered similar integrals in analyzing dissipation in microstrip lines with infinite edge currents and was able to circumvent the problem by halting the integral at a distance δ from the edge and comparing the conductor loss of the thin microstrip line (modeled as a zero thickness line) with that of a finite thickness strip [5]. The procedure for determining the stopping distance δ was generalized to different edge shapes by Barsotti et al. [6]. Following Lewin, to include the conductor loss in MOM_2 for more accurate analysis of reflectarrays, we derive a stopping distance δ for evaluating the divergent integrals

Received 26 July 2018, Accepted 5 November 2018, Scheduled 11 November 2018

* Corresponding author: Sembiam R. Rengarajan (srengarajan@csun.edu).

[1] Department of Electrical and Computer Engineering, California State University, Northridge, CA 91330, USA. [2] Jet Propulsion Laboratory, California Institute of Technology, Pasadena, CA 91109, USA.

by equating the conductor loss calculated in MOM_2 to that in MOM_1 The stopping distance thus derived is found to work for a wide range of parameters of reflectarrays, consisting of rectangular patches in this paper.

2. DIVERGING INTEGRALS

The integral equation for the induced current in a rectangular patch in a unit cell of an infinite array, using the Leontovich boundary condition, is given by

$$-\vec{E}_t^s + Z_m \vec{J} = \vec{E}_t^i \tag{1}$$

where $\vec{E}$ is the electric field, $\vec{J}$ is the surface current, Z_m is the intrinsic impedance of the patch conductor, the subscript t stands for the tangential component and the superscripts s and i stand for the scattered and the incident fields respectively. The scattered field is determined from an integral containing the Green's function and the patch current [1]. MoM expresses the unknown currents in terms of a set of basis functions and performs the inner product of both sides of (1) with each testing function, which is the same as the basis function in the Galerkin process, thus yielding a set of simultaneous equations. Equations containing the inner product of the mth testing function, denoted by the subscript m, are

$$\langle -\vec{E}_x^s(J_x), J_{xm}\rangle + \langle -\vec{E}_x^s(J_y), J_{xm}\rangle + Z_m\langle J_x, J_{xm}\rangle \;=\; \langle E_x^i, J_{xm}\rangle \tag{2}$$

$$\langle -\vec{E}_y^s(J_x), J_{ym}\rangle + \langle -\vec{E}_y^s(J_y), J_{ym}\rangle + Z_m\langle J_y, J_{ym}\rangle \;=\; \langle E_y^i, J_{ym}\rangle \tag{3}$$

The basis function for the x-directed electric current in MoM_1 is given by

$$\cos(\pi x/a)[1-(2x/a)^2]^{-1/2} \tag{4}$$

where a is the patch length along x (see Fig. 1). Its width along y is b [2]. The expressions for the y-directed current has a similar variation with x and a replaced by y and b, respectively. The basis functions for J_x in MoM_2 are in the form

$$\begin{pmatrix} \cos(m\pi x/a) \\ \sin\{(m+1)\pi x/a\} \end{pmatrix} \begin{pmatrix} \cos(n\pi y/b) \\ \sin\{(n+1)\pi y/b\} \end{pmatrix} \cdot [1-(2x/a)^2]^{-1/2}[1-(2y/b)^2]^{-1/2} \tag{5}$$

where $m = 1, 3, 5$ etc. and $n = 0, 2, 4$ etc. It is found that two odd and two even variations along each direction yield excellent accuracy with sixteen unknown coefficients for a non-separable distribution for J_x. For the y-directed current, the basis functions can be found by replacing x, y, a, and b by y, x, b, and a respectively. In Eqs. (2) and (3) the last term on the left containing the inner product of basis functions and testing functions will diverge for MoM_2 whereas it converges for MoM_1.

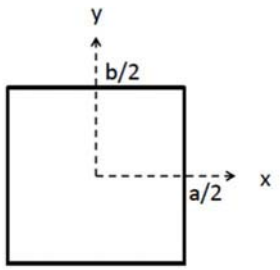

Figure 1. A rectangular patch in the unit cell of an infinite reflectarray.

3. COMPUTED AND MEASURED RESULTS

Table 1 shows the parameters of reflectarray antennas discussed in this paper. The stopping distance δ was varied until the calculated value of the conductor loss at resonance in MoM_2 agreed with the

Table 1. Reflectarray parameters for two cases.

Parameters	Case A	Case B
Nominal resonant frequency	35.75 GHz	13.285 GHz
Lattice spacing	0.4191 cm	1.1291 cm
Substrate thickness	0.0381 cm	0.08128 cm
Substrate dielectric constant	2.9503	3.58
Loss tangent	0.0012	0.0027
Angles of incidence of the plane wave (θ, ϕ)	(0°, 0°)	(30°, 0°)

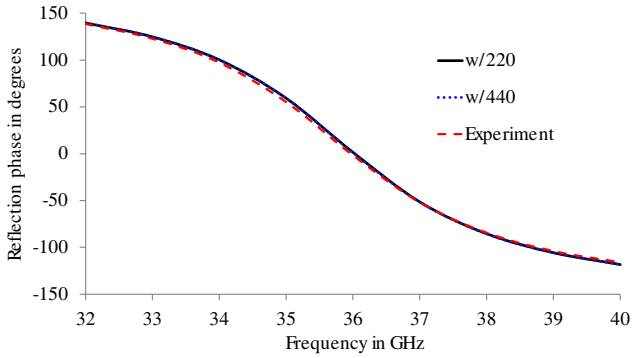

Figure 2. Computed and measured values of the reflection coefficient phase for $\delta = w/220$ and $\delta = w/440$ (Case A).

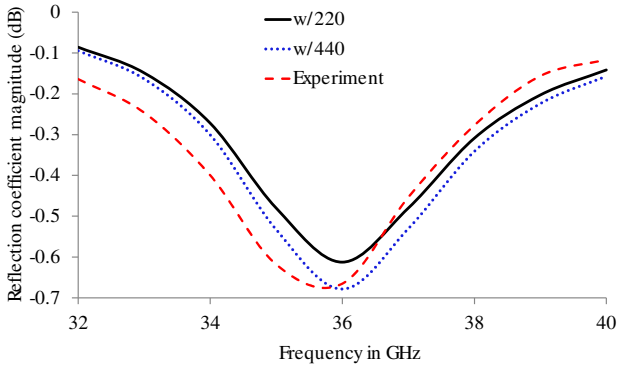

Figure 3. Computed and measured values of the reflection coefficient magnitude for $\delta = w/220$ and $\delta = w/440$ (Case A).

corresponding result in MoM_1. Conductor loss computed by MoM_1 has previously been shown to be accurate [1]. Reflectarray parameters shown in Case A of Table 1 with square patches of side 0.2162 cm were employed in this exercise. The value of δ is found to be $w/220$, where w, the width is b for J_x and a for J_y. Figs. 2 and 3 show the computed values of the reflection coefficient phase and magnitude, respectively, for two different values of δ. The reflection coefficient phase is independent of δ whereas the magnitude decreases with δ. Excellent agreement between computed and measured values is found for the phase in Fig. 2. We found that a value of $\delta = w/440$ produces a slightly better agreement with experimental results for the magnitude of the reflection coefficient over the frequency band of 32 to 40 GHz in Fig. 3. However, a value of $\delta = w/220$ is used in this work, since it exhibits better results for all cases, including obliquely incident plane waves, discussed later. Theron and Cloete's calculations for the conductor loss show that the use of Leontovich boundary condition can introduce error, but provides a conservative approximation that is useful in engineering practice [7]. Also, the discrepancy between theory and experiment for the conductor loss is found to be greater than 0.2 dB in [8]. Since the difference between MoM_2 and measured or HFSS [9] values of reflection coefficient magnitude is found to be within 0.1 dB in this work, the conductor loss computed using $\delta = w/220$ in MoM_2 is acceptable in designs and analyses of reflectarrays. We assumed the ground plane to be a perfect conductor and doubled the surface impedance of the patch, thereby equating the conductor loss in the rectangular patch to that of the ground plane. This simplified procedure, proposed in [3], is justified by the cavity model for a patch antenna [10].

Figure 4 shows the reflection coefficient magnitude at resonance as a function of substrate thickness for Case A. Square patches of side 0.2162 cm were used in this exercise. The resonant frequency given in Table 2 is found to decrease as the substrate thickness increases. A value of $\delta = w/220$ is used in MoM_2 in Fig. 4. The magnitude of the reflection coefficient computed by MoM_2 is found to be in very good agreement with that of MoM_1 for the substrate thickness down to 0.025 wavelength in the

Table 2. Resonant frequency in GHz as a function of substrate thickness for two different values of δ (case A in Table 1).

Substrate thickness mm	Resonant frequency $\delta = w/220$	Resonant frequency $\delta = w/440$
0.1954	37.830	37.825
0.3175	36.592	36.584
0.381	36.026	36.018
0.4396	35.539	35.532
0.4885	35.156	35.149

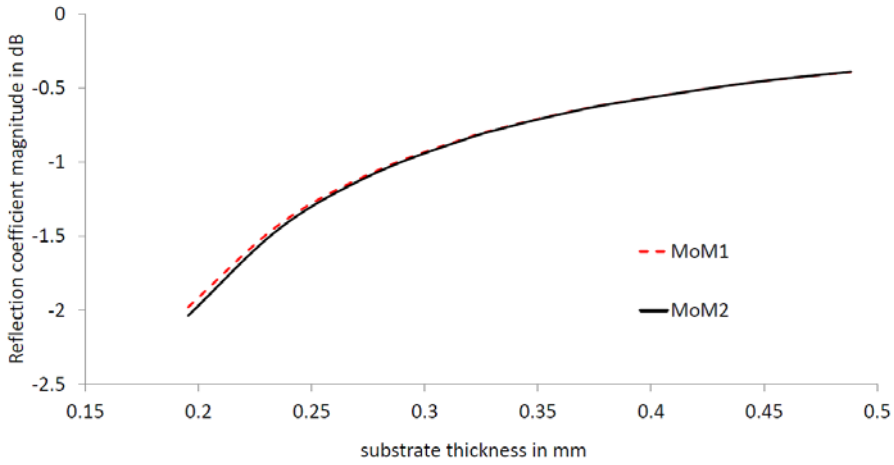

Figure 4. The reflection coefficient magnitude versus substrate thickness for Ka band.

substrate material [2]. The accuracy of MoM_1 is known to be poor for thin substrates that exhibit high values of losses. Computed values of the resonant frequency shown in Table 2 agree to within 0.02% for $\delta = w/220$ and $\delta = w/440$. Reflection coefficient magnitudes computed using $\delta = w/220$ in MoM_2 for other values of substrate permittivity, not shown here, also showed good agreement with the corresponding results of MoM_1.

Figure 5 shows the reflection coefficient magnitude at resonance versus substrate thickness for a Ku band reflectarray (Case B in Table 1). The side of each unit cell square patch is 0.542 cm. A TM to z plane wave is incident at an angle of $\theta = 30^\circ$ and $\phi = 0^\circ$.

Experimental results for this reflectarray were used to validate MoM_1 and MoM_2 for the TE polarization in a prior work [2]. The value of $\delta = w/220$ used here in MoM_2 for oblique incidence produces very nearly the same values of the reflection coefficient magnitude of MoM_1, even though the stopping distance was determined for normal incidence for the Ka band reflectarray. Figs. 4 and 5 show that the loss increases rapidly as the substrate thickness decreases below approximately 0.066 wavelength in the substrate material since the patches exhibit high quality factor.

Table 3 shows computed results for the resonant frequency and the total loss at resonance for reflectarrays of square patches of side 0.216 cm. All other parameters are specified in Table 1, case A. The results show that the resonant frequencies are independent of the dielectric loss tangent. The total loss computed by the two methods is in good agreement, thereby demonstrating that the stopping distance δ used in MoM_2 works for a wide range of values for the dielectric loss tangent as well.

Figures 6 through 11 show the reflection coefficient magnitude and phase as a function of frequency for the Ka band reflectarray (Case A in Table 1) with an added 0.0127 cm thick Kapton superstrate

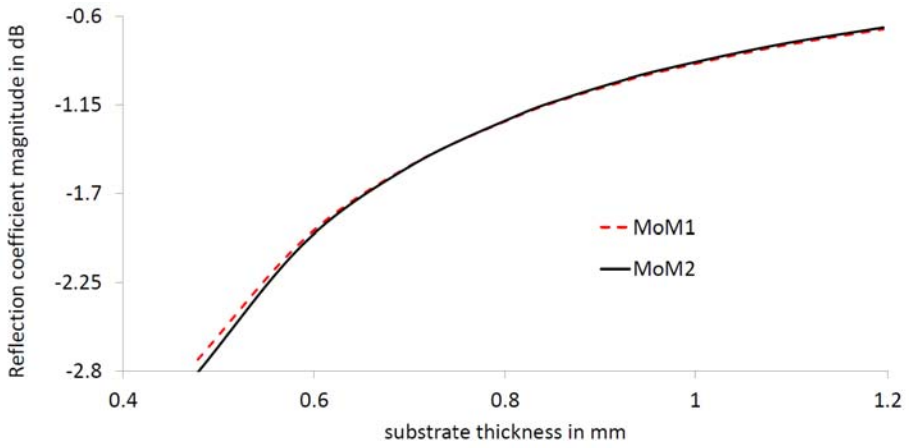

Figure 5. The reflection coefficient magnitude versus substrate thickness for Ku band.

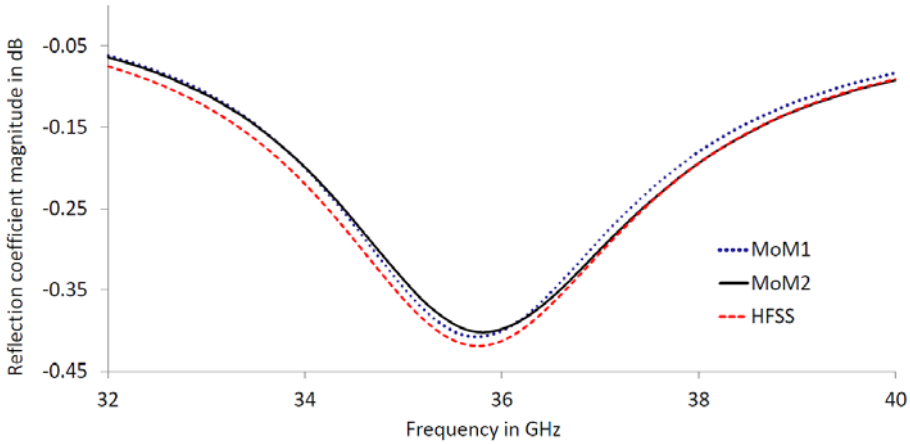

Figure 6. The reflection coefficient magnitude for a reflectarray with a superstrate at normal incidence.

layer of dielectric constant 3.0 and loss tangent 0.001. The square patch size is adjusted to a side length of 0.2025 cm in order to match the 35.75 GHz resonant frequency of the patch without substrate in Fig. 3. MoM_2 used with $\delta = w/220$ was also found to provide accurate results in all cases that included a superstrate. Figs. 6 and 7 show the results for the normal incidence. Figs. 8 and 9 correspond to $\theta = 45^\circ$ and $\phi = 0^\circ$ for TE polarization while Figs. 10 and 11 present the results for $\theta = 45^\circ$ and $\phi = 0^\circ$ for TM polarization. Very good agreement between MoM and HFSS are found for all cases. The

Table 3. Resonant frequency in GHz and total loss in dB as a function of the dielectric loss tangent for reflectarrays (case A in Table 1 with square patches of side 0.216 cm).

Dielectric loss tangent	MoM_1 Resonant Frequency	MoM_1 Total loss	Mom_2, $\delta = w/220$ Resonant Frequency	Mom_2, $\delta = w/220$ Total loss
0.0012	35.92	−0.61	36.03	−0.61
0.005	35.92	−1.20	36.03	−1.18
0.01	35.92	−1.98	36.03	−1.94
0.02	35.92	−3.56	36.00	−3.48

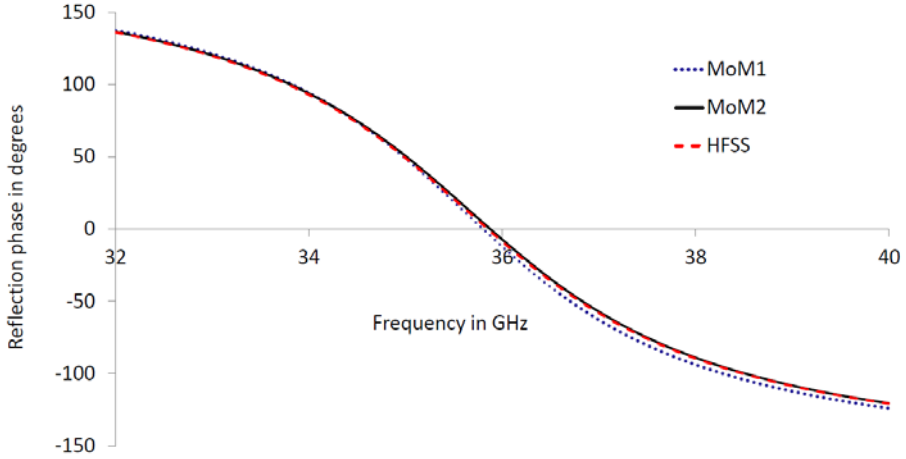

Figure 7. The reflection coefficient phase for a reflectarray with a superstrate at normal incidence.

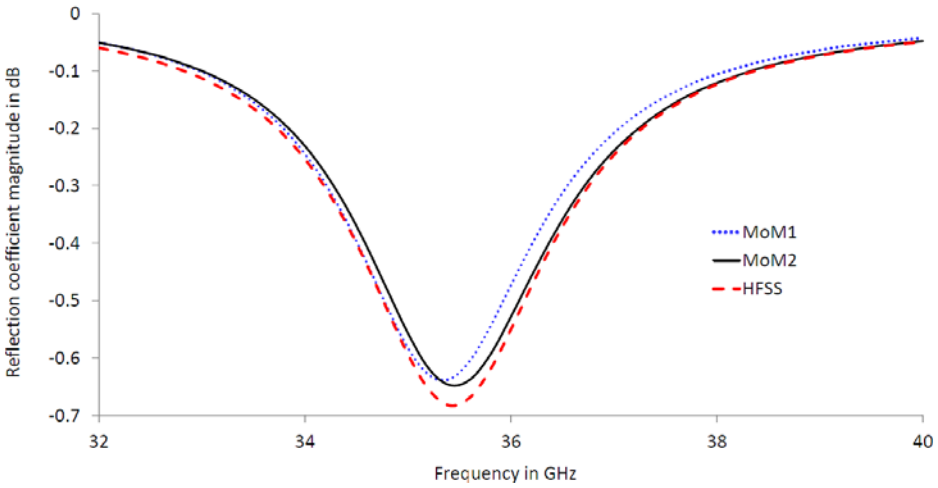

Figure 8. The reflection coefficient magnitude for a reflectarray with a superstrate for TE polarization at 45°.

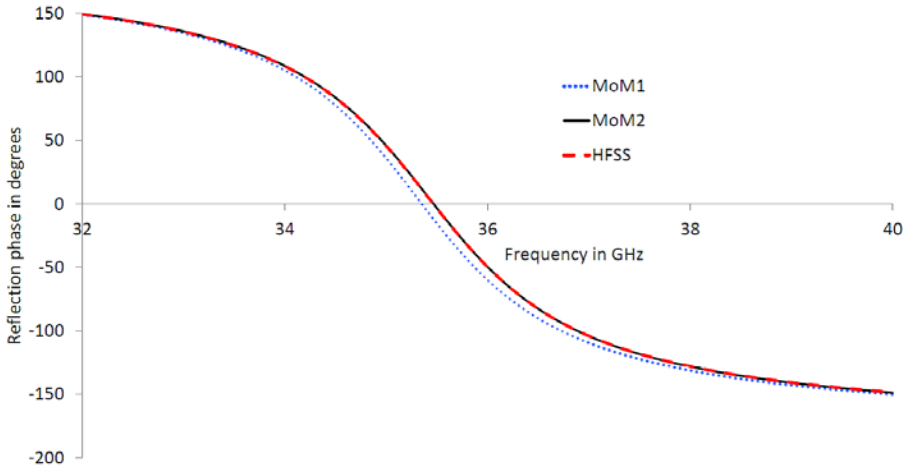

Figure 9. The reflection coefficient phase for a reflectarray with a superstrate for TE polarization at 45°.

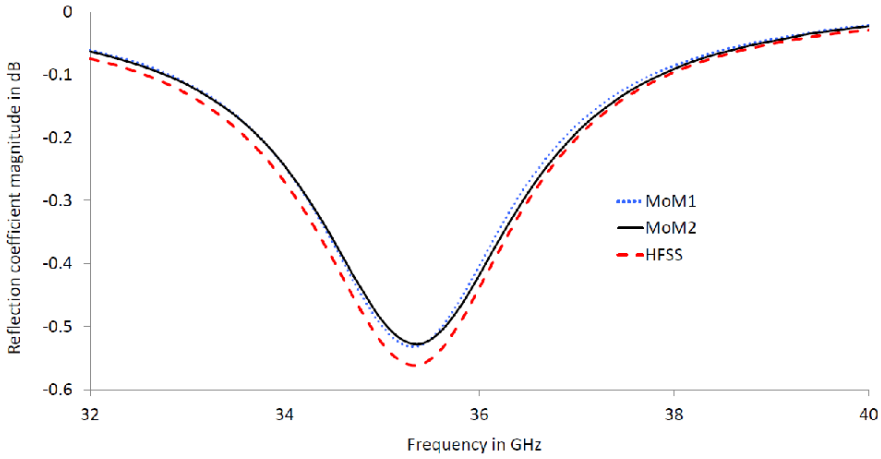

Figure 10. The reflection coefficient magnitude for a reflectarray with a superstrate for TM polarization at 45°.

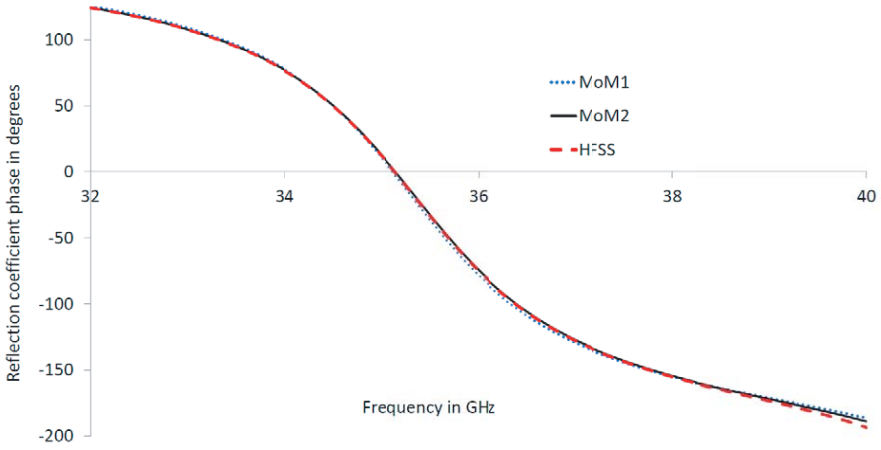

Figure 11. The reflection coefficient phase for a reflectarray with a superstrate for TM polarization at 45°.

discrepancy between MoM and HFSS for the reflection coefficient magnitude is typically within 0.1 dB in all cases. Results computed using MoM_2 are in better agreement with those of HFSS, especially for the reflection phase.

MoM_2 exhibits typically smaller than 0.1 dB lower loss than HFSS for all cases. The resonant frequencies computed by MoM_1 for all cases are within about 0.3% of the value computed by HFSS. MoM_2 is in excellent agreement with HFSS for resonant frequencies. Thus, the choice of $\delta = w/220$ is optimum for all cases of substrate thickness, permittivity, dielectric loss tangent, polarization, angles of incident plane waves and for superstrates as well.

4. CONCLUSION

For diverging integrals encountered in the Galerkin technique employing basis functions with edge conditions approaching infinity for reflectarrays consisting of thin rectangular patches, a stopping distance has been proposed. The use of such a stopping distance does not affect the reflection phase or the resonant frequency. It is found to work well, yielding reflection coefficient magnitude within 0.1 dB of measured or HFSS results for a range of values of dielectric constant, substrate thickness and for superstrates as well. The method of doubling the surface impedance of the patch to account for the loss in the ground plane has been found to be valid.

ACKNOWLEDGMENT

The authors wish to thank Dr. Matthew Radway and Dr. Jefferson Harrell for experimental results and Liza Ma for HFSS computations. Dr. Ronald J. Pogorzelski at California State University, Northridge, is thanked for helpful suggestions for the wording of parts of this paper. The research was carried out in part at the Jet Propulsion Laboratory, California Institute of Technology, under a contract with the National Aeronautics and Space Administration.

REFERENCES

1. Pozar, D. M., S. D. Targonski, and H. D. Syrigos, "Design of millimeter wave microstrip reflectarray," *IEEE Trans. Antennas Propag.*, Vol. 45, No. 2, 287–296, Feb. 1997.
2. Rengarajan, S. R., "Choice of basis functions for accurate characterization of infinite array of microstrip reflectarray elements," *IEEE Antennas Wireless Propag. Lett.*, Vol. 4, 47–50, 2005.
3. Mosig, J., "Arbitrary shaped microstrip structures and their analysis with a mixed potential integral equation," *IEEE Trans. Antennas Propag.*, Vol. 36, No. 2, 314–323, Feb. 1988.
4. Van Deventer, T. E., L. P. B. Katehi, and A. C. Cangellaris, "Analysis of conductor losses in high-speed interconnects," *IEEE Trans. Microw. Theory Techn.*, Vol. 42, No. 1, 78–83, Jan. 1994.
5. Lewin, L., "A method of avoiding edge current divergence in perturbation loss calculations," *IEEE Trans. Microw. Theory Techn.*, Vol. 32, No. 7, 717–719, Jul. 1984.
6. Barsotti, E. L., E. F. Kuester, and J. M. Dunn, "A simple method to account for edge in the conductor loss in microstrip," *IEEE Trans. Microw. Theory Techn.*, Vol. 39, No. 1, 98–106, Jan. 1991.
7. Theron, I. P. and J. H. Cloete, "On the surface impedance used to model the conductor losses of microstrip structures," *IEE Proceedings on Microwaves Antennas and Propag.*, Vol. 142, No. 1, 35–40, Feb. 1995.
8. Rajagopalan, H. and Y. Rahmat-Samii, "Dielectric and conductor loss quantification for microstrip reflectarray: simulation and measurements," *IEEE Trans. Antennas and Propag.*, Vol. 56, No. 4, 1192–1196, Apr. 2008.
9. http://www.ansys.com.
10. Richards, W. F., Y. T. Lo, and D. D. Harrison, "An improved theory for microstrip antennas and applications," *IEEE Trans. Antennas Propag.*, Vol. 39, No. 1, 38–46, Jan. 1991.